Tidal Mass Transfer in Elliptical-Orbit Binary Stars

Jeffrey T. Layton, John M. Blondin [1], Michael P. Owen

Department of Physics, North Carolina State University, Raleigh NC 27695-8202, USA

Ian R. Stevens

School of Physics and Space Research, University of Birmingham, Edgbaston, Birmingham B15 2TT, UK

Abstract

High mass X-ray binary star systems with elliptical orbits, like GX 301-2, often exhibit a peak in X-ray luminosity associated with periastron passage. We use a two dimensional hydrodynamics code to examine the possibility that these X-ray flares result from tidal stripping of gas from the primary star, and subsequent accretion of this gas onto the compact companion. We find that if the primary star is rotating near corotation with the orbiting compact companion at periastron, tidally stripped gas can accrete, causing X-ray flares. Such a tidally induced flare will occur substantially after periastron, at a phase of ~ 0.2 for the parameters used in our model. This flare is characterized by a brief disk accretion phase with a large angular momentum accretion rate. However, in our particular model this disk accretion phase was followed by an equally brief phase of accretion with the opposite sign of angular momentum, resulting in no long-term spin up of the X-ray pulsar.

Keywords: binaries: close; hydrodynamics; stars: mass-loss; X-rays: stars
PACS: 95.30.Lz; 97.10.Gz; 97.10.Me; 97.80.Jp

1 Introduction

X-Ray pulsar binary systems provide a valuable setting for the study of mass transfer in binary stars. The observed X-ray luminosity provides a measure of the mass accretion rate onto the compact object while the changes in pulse period reflect the accretion of angular momentum. Furthermore, the attenuation of the X-rays as inferred from the X-ray spectrum provides a measure

[1] 1996 Cottrell Scholar

of the distribution of circumbinary gas. Such systems are even more valuable when they possess non-circular orbits, for then we have the opportunity to study the mass transfer process under a well-defined experiment: a gradual change in the binary separation.

A number of X-ray binary systems, most of them Be X-ray binaries, are characterized by rather large orbital eccentricities. Many of these systems are X-ray transients, exhibiting distinct episodes of increased X-ray flux. These hard X-ray transients appear to exhibit at least two different types of temporal behavior. In one group are systems like X0115+63[0] which sometimes show an optical brightening preceeding a relatively long X-ray outburst with approximately linear decline. This association with optical transients suggests that the X-ray outburst is associated with some type of event occurring on the primary (Be) star. In another case, X-ray flares are separated by a relatively constant time interval consistent with the inferred orbital period of the binary system, suggesting instead that the X-ray flares are related to the orbital dynamics of the neutron star. In at least one system, A 1907+09[0], an orbital modulation can be seen on top of the long linear rise and fall of an extended outburst lasting several orbital periods. Parmar et al.[0] list six Be X-ray binaries for which the X-ray flaring interval is at least consistent with the orbital period of the system. At least three systems exhibit X-ray flares occurring close to periastron passage: V 0332+53[0], A 0538-66[0], and GX 301-2[0,0,0].

Perhaps the best studied elliptical-orbit X-ray pulsar is GX 301-2. The orbit of this system has a period of 41.5 days and an eccentricity of $\epsilon = 0.47$[0]. The X-ray flux exhibits periodic flares associated with periastron passage, although the flares occur about 1.4 days before periastron[0,0]. At a distance of 1.8 kpc, the peak X-ray luminosity is $\sim 10^{37}\mathrm{erg\,s^{-1}}$, compared to a quiescent flux roughly 10 times smaller. There is another periodic flare near apastron seen in BATSE data folded at the orbital period[0,0]. The peak flux of the apastron flare is ~ 4 times smaller than that of the periastron flare. One also sees two flares per orbit in A 1907+09[0,0].

The X-ray pulse period of GX 301-2 also shows some unusual behavior, with an extended epoch of essentially no net change in period from 1975 to 1985 followed by an epoch with fairly steady spin up[0]. Recent analysis of BATSE data have shown that the long-term spin up trend may be explained by individual episodes of spin up lasting roughly half an orbital period, but occurring only once every one or two years[0].

Early optical observations[0] identified the primary star, Wray 977, as a B2 Iae supergiant of radius $R_p = 43R_\odot$, mass $M_p = 25 - 35M_\odot$ (assuming that the mass of the neutron star $M_n = 1.4M_\odot$), and a distance $d = 1.8$kpc. With these parameters, they concluded that the primary is unlikely to fill its Roche lobe at any orbital phase and that GX 301-2 is a wind-fed system.

This conclusion naturally lead to the suggestion that the X-ray flares observed in GX 301-2 could be explained by the eccentric binary orbit model of Avni, Fabian, & Pringle[0]. In this model the X-ray luminosity is modulated by the changing wind conditions as the accreting neutron star moves through its eccentric orbit. Near periastron the stellar wind is slower and denser, leading to a higher mass accretion rate and hence higher X-ray luminosity compared to apastron. These models provided reasonably good fits to the X-ray light curve, although they could not reproduce a peak luminosity occurring ~ 1.4 days before periastron[0,0].

More recent attempts to model the X-ray light curve have resorted to the inclusion of a gas stream, both to augment the wind accretion and to provide the observed dependence of column density on orbital phase[0,0]. The results of this modeling thus suggest that tidal stripping from the surface of the primary star may play a role in the mass transfer process. The possibility that mass transfer is at least augmented by tidal stripping near periastron is also supported by new optical observations of Wray 977. Recently, Kaper et al.[0] have shown that the optical spectrum of Wray 977 is similar to that of ζ_1 Sco, a B1.5 Ia+ "hypergiant". Based on this comparison, they suggested a reclassification of Wray 977 to B1 Ia+, and a corresponding change in parameters to $M_p = 50 M_\odot$, $R_p = 70 R_\odot$, and $d = 5.3$kpc. These parameters suggest that the volume of the star may be larger than its tidal lobe near periastron, allowing for the possibility of mass transfer via tidal lobe overflow.

Tidal stripping near periastron has also been suggested for A 0538-66[0], another X-ray binary with a relatively large eccentricity ($\epsilon = 0.7$[0]). Stevens[0] modeled the X-ray light curve of A 0538-66 in terms of accretion from a tidally enhanced stellar wind; the tidal effects of the neutron star near periastron lead to a stronger, slower wind and hence a larger accretion-driven X-ray flux. Mavromatakis & Haberl[0] argue that the stream model of Haberl[0] fits the light curve of the two outbursts observed from A 0538-66 by ROSAT in late 1990.

While the modeling of Leahy[0] and Haberl[0] suggests the presence of a gas stream in GX 301-2, the existence of a tidally produced stream and its properties requires multidimensional hydrodynamic simulations. Along these lines, Boyle & Walker[0] computed the trajectories of test particles (with some crude modifications to account for hydrodynamic interaction) from the surface of a primary star in an eccentric orbit. They found that the tidally stripped gas can accrete onto the compact companion provided that the primary star was rotating with an angular velocity comparable to the orbital velocity near periastron, a requirement previously pointed out by Petterson[0].

The goal of this paper is to determine whether the observed X-ray flares in elliptical-orbit X-ray binaries can be interpreted in terms of wind accretion augmented by tidal lobe overflow at periastron. As a specific example, we base our hydrodynamical model on the parameters for GX 301-2.

2 The Numerical Model

To simulate the tidal mass transfer in elliptical-orbit X-ray binaries we employed the numerical model developed by Blondin et al.[0]. The current version of this model uses the hydrodynamics code VH-1 (http://wonka.physics.ncsu.edu/pub/VH-1), based on the piecewise parabolic method (PPM) of Colela & Woodward[0]. The model includes the gravity of both binary components, the rotation of the binary system, tidal distortion of the primary star, a radiatively driven wind from the primary star (using the Sobolev approximation), photoionization and heating of the circumbinary gas by the accretion driven X-rays, and radiation pressure due to the X-ray flux. Recent modifications to this numerical model[0] include improved boundary conditions at the surface of the primary, and attenuation of the X-ray flux by circumbinary gas.

The simulation is computed in a non-inertial frame in instantaneous corotation with the orbital system such that the neutron star remains at a fixed angular coordinate on the numerical grid, but changes position in the radial coordinate.

We assume that the surface of the primary is an equipotential surface whose volume is conserved throughout the orbit, and that the primary's axis of rotation is aligned with the axis of orbital rotation of the system. This first assumption requires that the primary star can respond instantaneously to the changing binary potential. Koh et al.[0] argue that this is a reasonable assumption for Wray 977 based on the analysis of tidal excitations by Kumar, Ao, & Quataert[0]. For the purposes of this project we have assumed that the primary's volume is equal to the volume of the critical lobe at periastron. Thus the primary is marginally overflowing its tidal lobe at periastron, but is underfilling at all other orbital phases. In a system with the center of mass at the origin, the primary at $\mathbf{r_1}$ and the neutron star at $\mathbf{r_2}$, the potential for a parcel of gas at a position $\mathbf{r}$ with respect to the center of mass of the system is given by:

$$\Phi = -\frac{GM_p}{|\mathbf{r}-\mathbf{r_1}|} - \frac{GM_n}{|\mathbf{r}-\mathbf{r_2}|} - \frac{1}{2}\omega^2 r_{bin}^2 - \frac{1}{2}({\omega_p}^2 - \omega^2) r_{pole}^2 \quad (1)$$

where ω is the instantaneous angular velocity of the system and ω_p is the rotational angular velocity of the primary, r_{bin} is the distance from the rotational axis of the binary system and r_{pole} is the distance from the rotational axis of the rotating primary.

In practice these assumptions required us to first find the volume of the equipotential surface of the critical lobe at periastron, and fix this as the volume of the star. Once this volume was calculated, a root finding method was employed to find the effective potential of an equipotential surface with this same volume for 200 equally spaced values of the binary separation between periastron and apastron. This data was then stored in a table for use by the hydrodynamic code, which computed the boundary of the primary star in the orbital plane based on the tabulated value of the surface potential.

The numerical grid consisted of a two dimensional circular polar grid with 251 angular zones and 400 radial zones, in a reference frame centered on the center of mass of the system and corotating with the neutron star. The first 100 radial zones are equally spaced a distance of 2.0×10^{10} cm, and the last 300 grow consecutively larger, with each being 1.006 times the size of the previous zone. The angular width of the zones starts at 2.8×10^{-3} radians at the location of the neutron star, and is similarly zoomed by a factor of 1.028. This grid provides high resolution at the surface of the primary in order to resolve the tidally distorted atmosphere, as well as in the vicinity of the accreting neutron star.

The radiative driving of the stellar wind from the primary star was treated in the Sobolev approximation following the model of Castor, Abbott, & Klein[0]. The "CAK" parameters of $\alpha = 0.53$ and $k = 0.12$ were estimated from Pauldrach, Puls, & Kudritzki[0] based on the effective temperature of Wray 977 of $T_{eff} \approx 22,000$K. The resulting terminal wind velocity and mass loss rate were $v_\infty \approx 1,000\,\mathrm{km\,s^{-1}}$ and $\dot{M}_w \approx 2 \times 10^{-6}\,\mathrm{M_\odot\,yr^{-1}}$, although they depended slightly on the assumed stellar rotation rate.

The X-ray luminosity of the neutron star was computed from the instantaneous mass accretion rate, $\dot{M}_x$, assuming an efficiency of 0.05: $L_x = 0.05\dot{M}_x c^2$. At each timestep the mass within the zone centered on the neutron star was removed from the numerical grid. In order to determine the mass accretion rate however, one must assume something about the dimension of the accreting region perpendicular to the orbital (computational) plane. We assumed a characteristic height of 2×10^{10} cm, a reasonable guess in the case of disk accretion. However, this will greatly underestimate the mass accretion rate in the case of wind accretion, where gravitational focussing in the third dimension is important.

Table 1
Parameters Used in Model

$M\prime$	$52 M_{\odot}$
M_n	$1.4 M_{\odot}$
e	.47
P_{orb}	41.5 days
T_{eff}	$2.2 \times 10^4 K$

3 Results

We ran two simulations for GX 301-2, each with a different rotation rate for the primary. Observational evidence favors a slow rotation with a period comparable to the orbital period[0], so for our first (slow) model we chose a rotation rate for the primary of $\omega_p = 2\pi/P_{orb}$. Since Boyle & Walker[0] argue the need for a fast rotation rate, we ran a second (fast) model with a rotational velocity equal to the orbital velocity at periastron, $\omega_p = 2\pi[(1+\epsilon)^{1/2}/(1-\epsilon)^{3/2}]/P_{orb}$. The other parameters used in the model are based on the parameters for GX 301-2 derived by Kaper et al.[0], which are more consistent with the tidal overflow model being investigated here. These parameters are listed in Table 1.

3.1 Case I: Slow Rotator

In the first model, the rotation period of the primary was set to the orbital period of 41.5 days. As such, the rotation of the primary star lags far behind the orbiting neutron star during periastron passage. Petterson[0] pointed out that in such circumstances tidally stripped gas will have insufficient specific angular momentum to reach the neutron star. The animations shown in Figure 1 confirm this; mass transfer remains in the wind accretion mode throughout the orbit. A small tidal stream briefly forms during periastron passage, but most of this mass falls back to the surface of the primary as the neutron star recedes from it.

The X-ray light curve, shown in Figure 2, exhibits a broad peak in L_x from slightly before periastron to phase 0.12. The peak luminosity reaches $L_x \approx 10^{35} \mathrm{erg\,s^{-1}}$, compared to $L_x \approx 5.0 \times 10^{33} \mathrm{erg\,s^{-1}}$ far from periastron. This increase is the result of the strong enhancement of wind accretion near and after periastron. The stellar wind originating from the line of centers during periastron passage has a substantially lower velocity and higher mass loss rate than the undisturbed stellar wind, resulting in a larger wind accretion rate. In fact our numerical model underestimates this increase in wind accretion because of

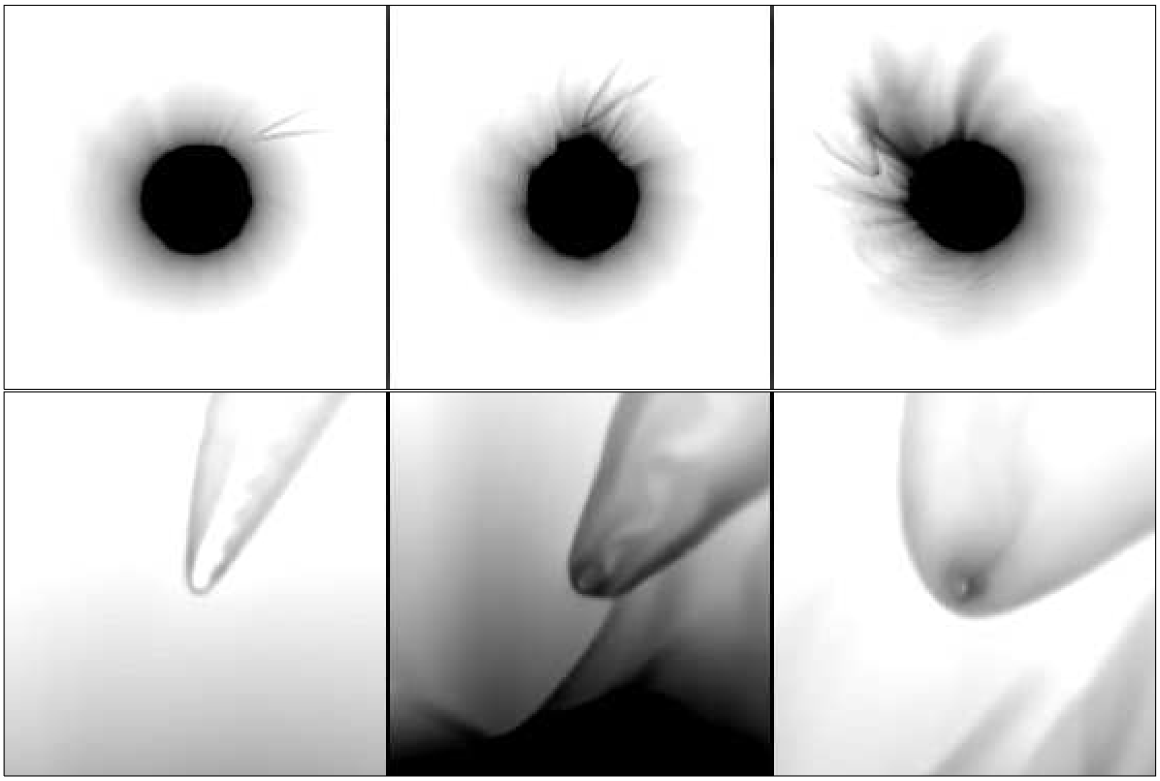

Fig. 1. Animations of the slow rotator model showing the entire orbital system (top) and a close up of the accreting neutron star (bottom). The animation shows slightly more than one orbit. The color scale (from red to dark blue) represents the gas density (from high to low) of the wind. The close up images are viewed in a rotating frame such that the primary star is always below the image shown.

our assumptions about the third dimension. The slower wind velocity results in a larger accretion radius than was assumed in the numerical model, with the result that the X-ray luminosity output by the model is a few times too low. Given this restriction, the height of the periastron peak (one order of magnitude) is uncertain, but the duration in orbital phase is expected to be reasonably accurate.

The angular momentum accretion rate, $\dot{J}$, remains low throughout the simulation. Away from periastron the sign of $\dot{J}$ is uniformly positive, although we note that the hydrodynamics of the wind accretion are poorly resolved during this part of the orbit. In the vicinity of periastron $\dot{J}$ shows clear oscillations in sign, with the result that there is virtually no net angular momentum accreted during periastron passage, as shown in the plot of accumulated angular momentum, J, in Figure 2. During this part of the orbit the wind velocity is lower, the accretion radius is higher, and the grid spacing is finer, such that the hydrodynamics of the wind accretion are adequately resolved. Given sufficient numerical resolution, we might expect the time-averaged value of $\dot{J}$ to remain approximately zero throughout the orbit, and not just during periastron passage.

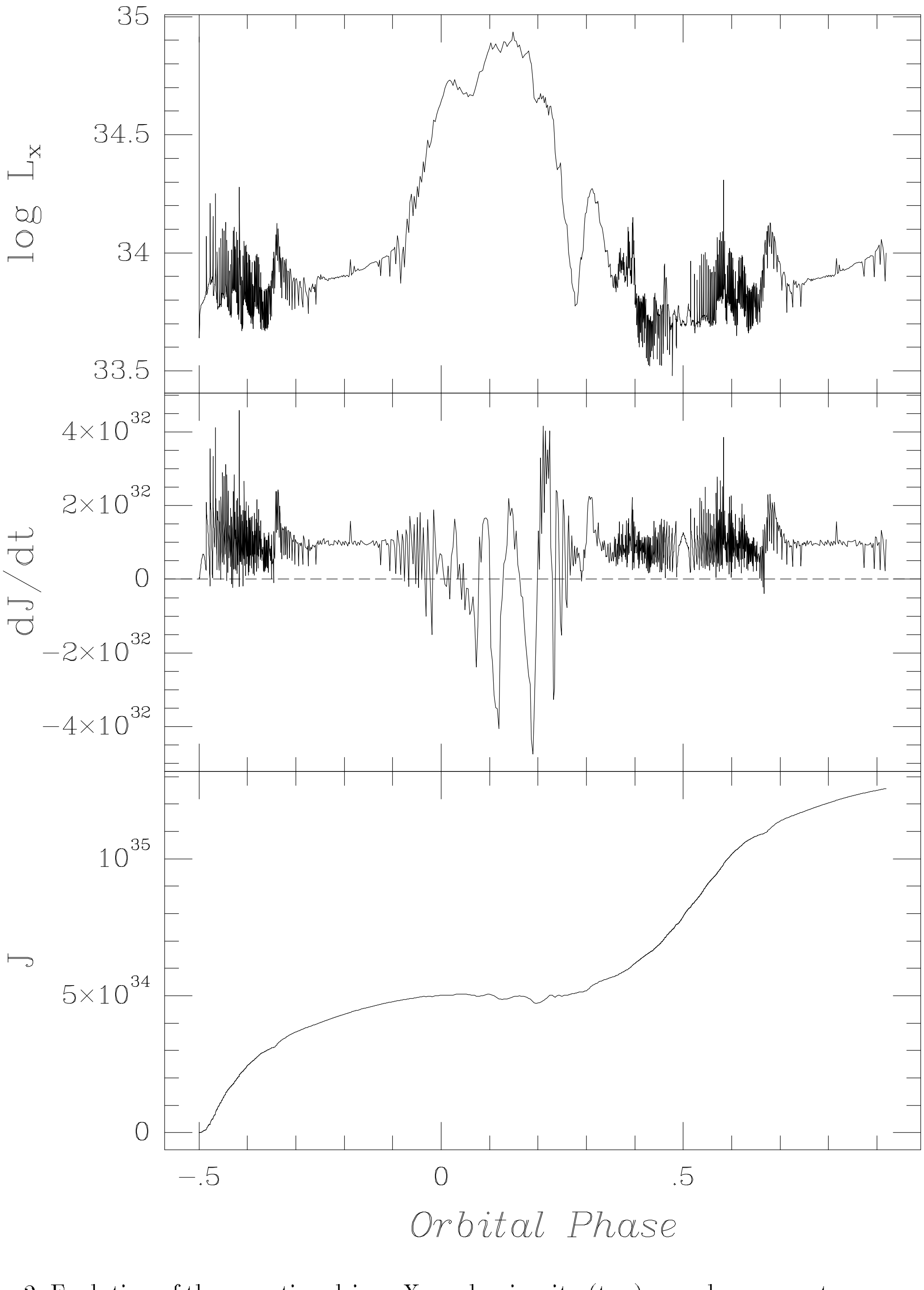

Fig. 2. Evolution of the accretion driven X-ray luminosity (top), angular momentum accretion rate (middle), and accumulated angular momentum of the neutron star (bottom) for the slow rotator model.

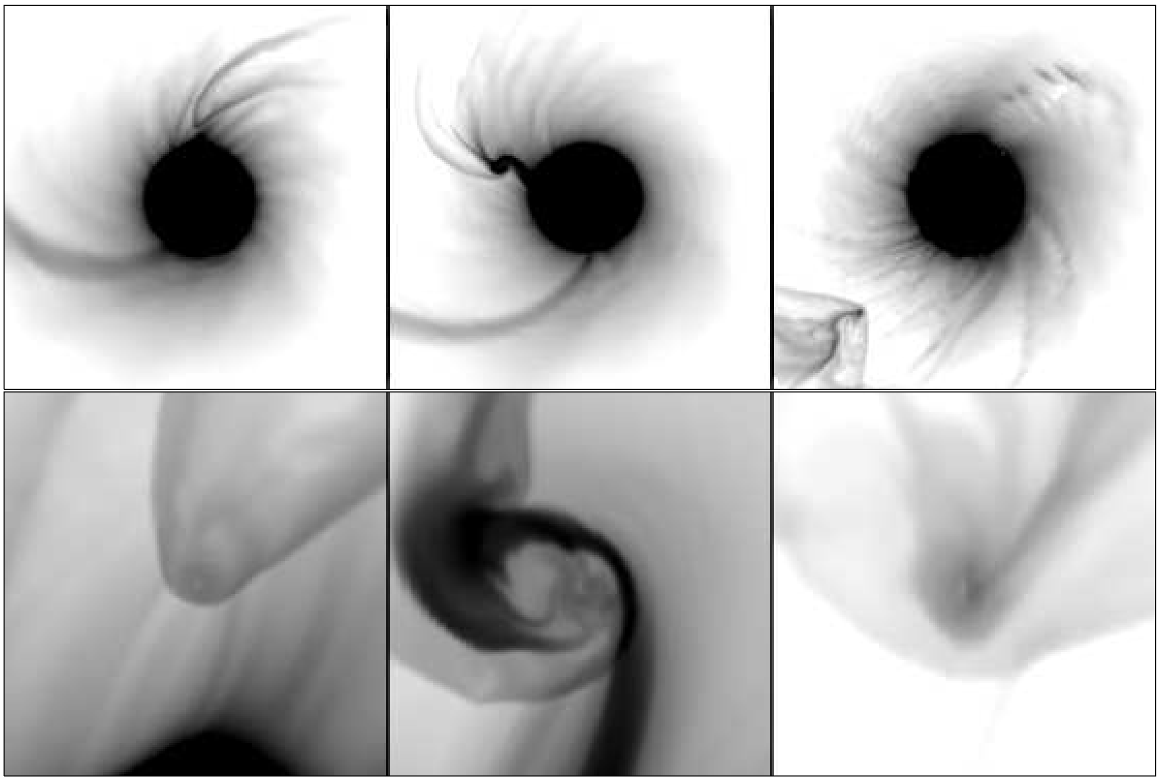

Fig. 3. Animations of the fast rotator model showing the entire orbital system (top) and a close up of the accreting neutron star (bottom), as in Figure 1. The animation shows roughly 1.7 orbits, corresponding to the latter half of the simulation (cf. Fig. 4).

3.2 Case II: Fast Rotator

In the second model the rotation of the primary star was adjusted such that the star was in instantaneous corotation with the neutron star at periastron. The appropriate rotational period is $P = 12.5$ days. In contrast to the first model, the model with faster stellar rotation did produce an accretion disk, as seen in Figure 3. A comparison of the two models (e.g., compare the close-up animations in Figs. 1 and 3) shows that the faster stellar rotation allows more material to be pulled off the surface of the primary and more of this material to reach the neutron star. The result is the formation of a well defined tidal stream leading to the presence of a transient accretion disk.

If it were not for the accretion disk, the X-ray light curve for the fast model, shown in Figure 4, would closely resemble the light curve for the slow model; A base luminosity of $\sim 10^{34}$ erg s^{-1} with a broad peak reaching luminosities roughly ten times larger. However, during the existence of the accretion disk, roughly from orbital phase 0.13 to 0.3, L_x soars to $\sim 10^{36}$ erg s^{-1}. This short duration of the accretion disk appears consistently in each orbit of the simulation.

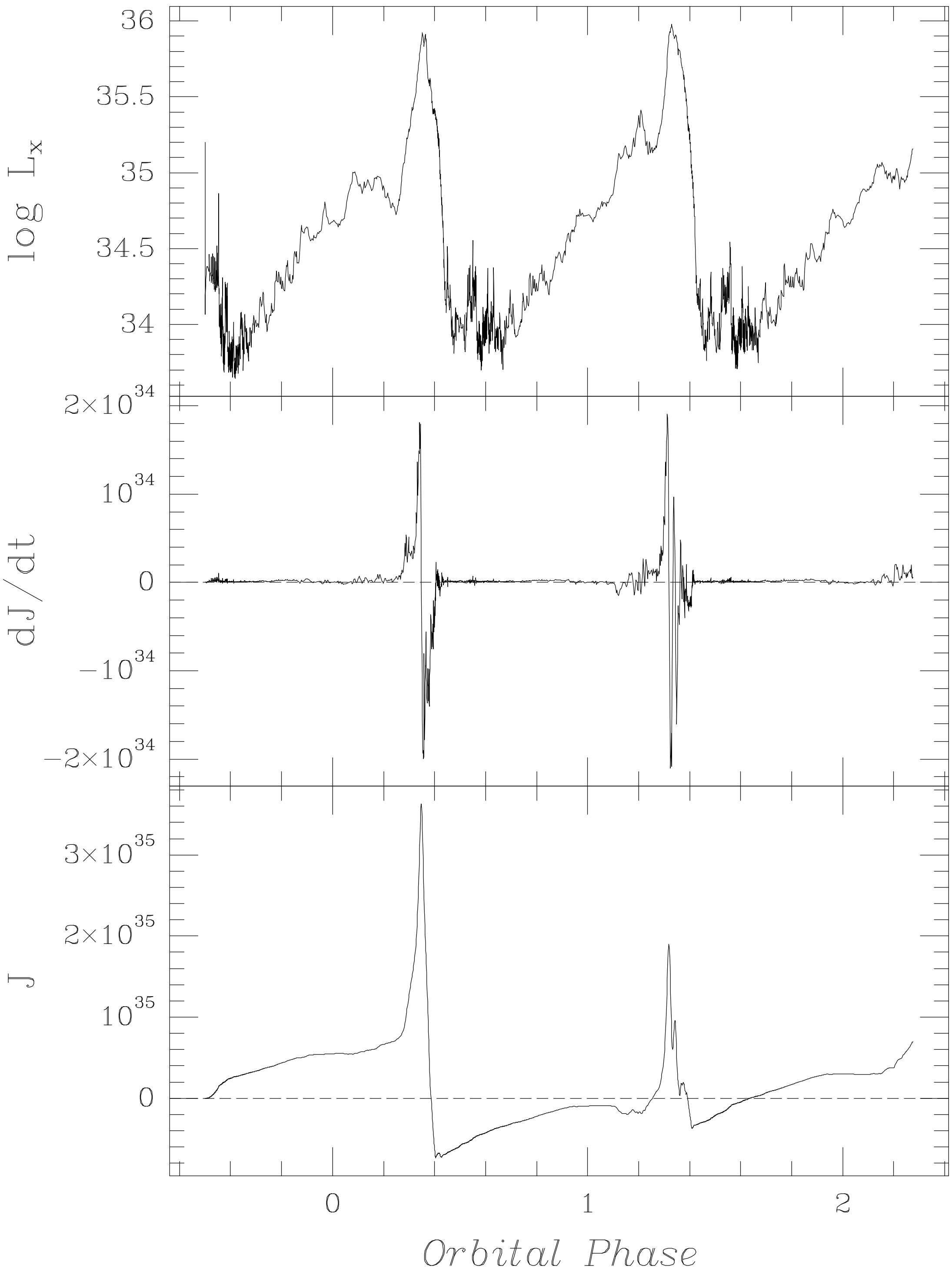

Fig. 4. Evolution of the accretion driven X-ray luminosity (top), angular momentum accretion rate (middle), and accumulated angular momentum of the neutron star (bottom) for the fast rotator model.

The accretion disk does not form until well after periastron because of the time necessary for the gas tidally stripped during periastron passage to reach the neutron star. The densest material pulled off the surface is moving with a radial velocity of only slightly more than 100 km s^{-1}, and hence requires at least a day to reach the neutron star. Even then it takes a significant amount of time for the gas to encircle the neutron star and begin accreting. Shortly after the disk forms, however, an interesting phenomenon occurs. The angular momentum accretion rate, although starting off positive when the disk forms, rapidly drops to negative values of comparable magnitude to the positive disk accretion rate. This sudden switching of the sign of $\dot{J}$ is shown in Figure 4, where we also plot the accumulated angular momentum, J. From this latter plot one can see that the total amount of angular momentum accreted with opposite rotation is comparable to, and indeed for the first orbit larger than, the total angular momentum accreted with positive rotation. This switch in the direction of rotation of the accreting material coincides with the peak in the mass accretion rate.

The antirotation of the accreting material appears to be driven by the passage of tidally enhanced wind as the motion of the neutron star slows down with respect to the rotation of the primary star. In a circular orbit system the gas flowing through the inner Lagrangian point has insufficient angular momentum to accrete directly onto the compact companion. Instead, the tidal stream approaches the accretor from behind (in the sense of orbital motion), as seen in the animations in Figure 3 near periastron. This in turn leads to accretion with positive values of $\dot{J}$ (i.e., in the same sense as the orbital angular momentum). In our fast rotator model, however, the wind can have comparable, or even more, angular velocity than the accretor during orbital phases other than periastron. As the tidally enhanced wind fades away following periastron, it also advances ahead of the neutron star, such that the net angular momentum approaching the neutron star changes sign. This process has the effect of "flushing" the material in the disk, producing a short phase of high L_x as the bulk of the gas in the transient disk is accreted on a short timescale, followed by low-L_x wind accretion.

4 Discussion & Conclusions

These simulations have shown that tidal stripping in eccentric-orbit X-ray binaries can produce periodic X-ray flares. Such flares are characterized by a large increase in X-ray luminosity occurring substantially after periastron passage by the accreting companion star. We have confirmed the results of Boyle & Walker[0], who found that mass tidally stripped from a star in an elliptical orbit cannot accrete onto the compact companion star unless the primary star is close to corotation at periastron. Moreover, we have demonstrated that a tidally produced gas stream from a star filling its critical lobe, in corotation at periastron, is found only after periastron passage. The assumptions of Haberl[0] and Leahy[0] are therefore not consistent with a tidally produced stream from the primary star.

Note that we do not consider nonequilibrium tides nor stars exceeding their critical potential lobe at periastron, both of which may modify our results. For example, one of our first attempts at simulating this system used inappropriate boundary conditions at the stellar surface leading to substantially more mass loss at periastron, as might be the case if the star exceeded its critical potential lobe at periastron. The result was a much more massive accretion disk that remained in orbit around the neutron star for roughly half the binary orbital period, producing an extended epoch (many days) of spin up reminiscent of the spin up episodes observed in GX 301-2 by BATSE. The recent BATSE results[0] suggest that most orbits result in zero net angular momentum accretion, as seen in our simulations presented here. The overall increase in spin rate observed since 1984 is then attributed to isolated spin-up events that occur relatively infrequently (1 out of 10 to 20 orbits). These rapid spin-up events are likely the result of a temporary accretion disk, but whether these transient disks are formed through wind accretion or through tidal stripping as in the simulations shown here is not clear.

The referee [receiving editor?] has pointed out that our numerical result of no net accretion of angular momentum in tidal mass transfer has important consequences for the very fast rotation ($P = 0.069$ s) observed in A 0538-66[0]. However, as described in the preceeding paragraph, we beleive this result is closely tied to our model assumptions. Relaxing these assumptions, e.g., a primary exceeding its critical potential lobe at periastron, could conceivably lead to a net accretion of angular momentum and hence a fast rotator as in A 0538-66.

Overall, our simulations of tidal stripping do not provide an accurate quantitative match to the observed X-ray properties of GX 301-2. In particular, the tidally induced flares seen in our numerical models are characterized by an orbital phase near 0.2, well after periastron. In contrast, the X-ray flares of GX 301-2 occur significantly before periastron with a smaller flare occurring near apastron. We see no evidence in our simulations that tidal stripping could lead to enhanced gas density in the wind that might affect accretion rates near apastron. Finally, measurements of line widths from Wray 977 suggest a rotation rate considerably slower than periastron corotation[0], yet our results suggest that a tidally produced X-ray flare can occur only if the mass-losing star is rotating close to corotation at periastron. Our work thus suggests that a model for the X-ray flares in GX 301-2 based on enhanced wind accretion, perhaps from an equatorial disk[0,0], is more likely than one based on tidal stripping at periastron.

Although we have attempted to include a substantial amount of physics in our simulations, they remain highly idealized. Perhaps the most drastic restriction has been that of only computing flow in the orbital plane. This severely limits our ability to compute the accretion-driven X-ray luminosity, and hence the effects of this X-ray flux on the dynamics of the wind accretion process. A related limitation of our models is the relatively poor spatial resolution in the vicinity of the accreting neutron star, particularly away from periastron. Both of these problems conspire to limit our ability to accurately model wind accretion, although this was not the focus of our investigation. Note, however, that this means this model was not adequate to address the hypothesis of Chichkov et al.[0], who suggested that the influence of the wind-accretion driven X-rays can modify the accretion process to produce the observed X-ray light curve. Nonetheless, we believe our primary conclusions are independent of the limitations of our model: a tidally produced X-ray flare can occur only if the mass-losing star is rotating nearly synchronously at periastron, and such a flare will occur substantially after periastron.

Acknowledgement

This research was supported in part by NASA grant NAG 5-3110 and a Cottrell Scholars Award from the Research Corporation. J.T.L. acknowledges support from the NSF Research Experiences for Undergraduates program funded through the American Astronomical Society. The numerical simulations described in this paper were computed on a Cray T90 at the North Carolina Supercomputing Center.

References

[1] Avni, Y., Goldman, I. 1980, A&A, 90, 44

[2] Blondin J. M., Kallman, T. R., Fryxell, B. A., & Taam, R. E. 1990, ApJ , 356, 591

[3] Brown, J. C., & Boyle, C. B. 1984, A&A, 141, 369

[4] Boyle, C. B., & Walker, I. W. 1986, MNRAS, 222, 559

[5] Castro, J. I., Abbott, D. C., & Klein, R. I. 1975, ApJ, 195, 157

[6] Colella, P., & Woodard, P. R. 1984, J. Comput. Phys., 54, 174

[7] Chichkov, M. A., Syunyaev, R. A., Lund, I. Y., Brandt, S., & Castrotirado, A. 1995, Soviet Ast. Lett., 21, 435

[8] Haberl F. 1991, ApJ, 376, 245

[9] Kaper, L., Lamers, H.J.G.L.M., Ruymaekers, E., van den Heuvel, E.P.J., & Zuiderwijk, E.J. 1995, A&A, 300, 446

[10] Koh, D. T., Bildsten, L., Chakrabarty, D., Nelson, R. W., Prince, T. A., Vaughn, B. A., Finger, M. H., Wilson, R. B., & Rubin, B. C. 1997, ApJ, 479, 933

[11] Kumar, P., Ao, C., & Quataert, E. 1995, ApJ, 449, 294

[12] Leahy, D. A. 1991, MNRAS, 250, 310

[13] Makishima, K., Kawai, N., Koyama, K., Shibazaki, J., Nagase, F., & Nakagawa, M. 1984, PASJ, 36, 679

[14] Marshall, N., & Ricketts, M. J. 1980, MNRAS, 193, 7P

[15] Mavromatakis, F. & Haberl, F. 1993, A&A, 274, 304

[16] Mendelson, H., & Mazeh, T. 1991, MNRAS, 250, 373

[17] Owen, M. P., & Blondin, J. M. 1997, in preparation

[18] Pauldrach, A., Puls, J., & Kudritzki, R. P. 1986, A&A, 164, 86

[19] Parkes, G. E., Mason, K. O., Murdin, P. G., & Culhane, J. L. 1980, MNRAS, 191, 547

[20] Parmar, A. N., White, N. E., Stella, L., Izzo, C., & Ferri, P. 1989, ApJ, 338, 359

[21] Petterson, J. A. 1978, ApJ, 224, 625

[22] Pravdo, S. H., Day, C. S. R., Angelini, L., Harmon, B. A., Yoshida, A., Saraswat, P. 1995, ApJ, 454, 872

[23] Sato, N., Nagase, F., Kawai, N., Kelley, R. L., Rappaport, S., White, N.E. 1986, ApJ, 304, 241

[24] Skinner, G. K. et al. 1982, Nature, 297, 568

[25] Stella, L., White, N. E., Davelaar, J., Parmar, A. N., Blissett, R. J., & van der Klis, M. 1985, ApJ, 288, L45

[26] Stevens, I. R. 1988, MNRAS, 232, 199

[27] Watson, M. G., Warwick, R. S., & Corbet, R. H. D 1982, MNRAS, 199, 915

[28] White, N. E., & Swank, J. H. 1984, ApJ, 287, 856